Available online at www.sciencedirect.com
SCIENCE DIRECT
ELSEVIER
International Journal of Machine Tools & Manufacture 46 (2006) 114–121
INTERNATIONAL JOURNAL OF MACHINE TOOLS & MANUFACTURE DESIGN, RESEARCH AND APPLICATION
www.elsevier.com/locate/ijmactool

The coolant penetration in grinding with a segmented wheel—Part 2: Quantitative analysis

T. Nguyen, L.C. Zhang*

School of Aerospace, Mechanical and Mechatronic Engineering, The University of Sydney, NSW 2006, Australia

Received 14 March 2005; accepted 5 May 2005
Available online 11 July 2005

Abstract

This paper develops a quantitative model to predict the power of coolant penetration into the grinding zone of a segmented wheel. The model accounts for the coolant properties and system design characteristics governing the penetration mechanism revealed by the theory established in Part 1 of this series study. By coupling with the author's previous mist formation analysis, the model offers a quantitative control guideline for the optimal use of grinding coolants.

Keywords: Coolant; Optimisation; Quantitative model; Segmented grinding wheel; Mist formation

1. Introduction

Thermal damage is one of the major problems in grinding where a workpiece experiences heating within a small wheel-workpiece contact zone. Therefore, rapid convective heat dissipation within the zone is essential and it greatly depends on the quantity of coolant which can penetrate into the zone [1]. An understanding of the coolant penetration mechanism is therefore of particular importance in the development of an advanced coolant supply system. In Part 1 of this series study [2], the authors have explored the mechanisms of coolant penetration when using a conventional and a segmented wheel in surface grinding. It was found that unlike the conventional wheel, the segmented wheel possesses a higher pumping power when the wheel speed increases, and that the magnitude of the pumping power enhancement depends on the sum of velocities of the coolant jets. The significance in coolant minimisation [3] was qualitatively explained and proved to be possible under certain conditions, particularly when a pressurised coolant chamber was used. However, it must be emphasised that in practice, such applications usually involve complex flow geometries of the coolant jets influenced by two motions, the grinding wheel rotation and the coolant's radial motion [4]. These effects will significantly alter the development of the coolant velocity profile [5–8] which is a function of the grinding system configuration, total quantity of coolant supplied to the system and the viscous properties of coolant.

On the other hand, because of the interfacial instability, high speed coolant jets are more susceptibly disintegrated into drops [6,7]. The efforts to enhance the pumping power by simply increasing the jet velocity will raise the mist formation rate, as pointed out by the authors [4]. As these drops are intrusive to environment of manufacturing [9], a better solution for high pumping power must be associated with the environmental consciousness.

While the analytical modelling in Part 1 of this series study [2] reveals the mechanism of pumping power qualitatively, it is hard to produce a quantitative prediction with sufficient accuracy which is of great importance in practice. It is noticed that dimensional analysis can often give very satisfactory formulae for quantitative prediction, particularly when it is used in conjunction with an analytical model [10–16]. Thus, this paper will conduct a quantitative analysis of the pumping power to develop a guideline for the optimal use of coolant. The experimental setup is the same as in Part 1 of the series study [2]. The coolant jet velocity is determined by the method of high-speed strobe photography (see the Appendix for details).

* Corresponding author. Tel.: +61 2 9351 2835; fax: +61 2 9351 7060.
E-mail address: zhang@aeromech.usyd.edu.au (L.C. Zhang).

0890-6955/$ - see front matter © 2005 Elsevier Ltd. All rights reserved.
doi:10.1016/j.ijmachtools.2005.05.020

Nomenclature

A	area (m^2)
b	wheel width (m)
b_{ch}	inner coolant chamber width (m)
b_r	inner wheel rim width (m)
C_m, C_p	dimensionless correlation coefficients in Eqs. (17) and (21), respectively
C_f	coolant chamber characteristic coefficient ($1/m^4$)
C_{fw}	dimensionless geometrical influence number
C_s	coefficient in Eq. (2) (m^2)
d_h	perforated hole diameter (m)
d_l	break-up diameter of a liquid jet in Eq. (A1) (m)
f_c	centrifugal force acting on a unit volume of coolant (N/m^3)
g	gravitational constant (m/s^2)
h	equivalent liquid layer thickness in Eq. (2) (m)
l	break-up length of a liquid jet in Eq. (A1) (m)
N	total number of segments in a segmented wheel
n_{ch}	number of perforated holes within the coolant chamber (Fig. 5)
OES	occupational exposure standard (kg/m^3)
Oh	Ohnesorge number, Eq. (A3), $(Oh=\mu/(\rho\sigma d_l)^{0.5})$
P	pumping power (W)
P_{min}	minimum pumping power required (W)
P^*	power number, $(P/\rho R^5\omega^3)$
p	pressure (Pa)
Q	total coolant flow rate supplied to a system (m^3/s)
Q^*	flow rate number, Eq. (21), $(Q/R^3\omega)$
Q_m	mist flow rate (m^3/s)
$Q_{m,max}$	allowable mist flow rate (m^3/s)
Q_m^*	mist flow rate ratio in Eq. (21)
Q_{max}	maximum coolant flow rate required in Eq. (27) (m^3/s)
Q_{min}	minimum coolant flow rate required in Eq. (27) (m^3/s)
R	wheel radius (m)
Re	Reynolds number, $(\rho R^2\omega/\mu)$
Re_l	Reynolds number, Eq. (A4), $(\rho v_{ik} d_l/\mu)$
Re_c	critical Reynolds number, Eq. (A5)
v_{ik}	velocity of a coolant jet (m/s)
We	Weber number, $(\rho R^3\omega^2/\sigma)$
We_l	Weber number, Eq. (A2), $(\rho v_{ik}^2 d_l/\sigma)$
Δp	pressure drop
$\Delta\bar{p}_o$	mean static pressure drop through the perforated holes
Δz	perforated hole length shown in Fig. 3 (m)
X_m, X_p	dimensionless grinding variable, defined in Eqs. (18) and (21), respectively
γ	control volume angle (rad)
μ	dynamic viscosity (Ns/m^2) coolant density (kg/m^3)
ρ	coolant density (kg/m^3)
ρ_a	density of chemical additives (kg/m^3)
σ	surface tension (N/m)
ϕ	alignment angle of the fluid chamber in Fig. 4b (rad)
ω	rotational grinding wheel speed (rad/s)
ω_{max}	safety limit of grinding wheel speed (rad/s)

Superscripts

*	dimensionless number
m, n, q, r	correlation power factors

Subscripts

1 and 2	corresponding to planes 1 and 2, respectively
c	centrifugal
ch	coolant chamber
h	perforated hole of the segmented wheel
k	individual
m	mist
max	maximum
min	minimum
o	static
op	optimised
p	pumping power

2. Pumping power

2.1. Dimensional analysis

As shown in Figs. 1 and 2, the coolant layer, due to the wheel rotation, ω, is forced to penetrate into the wheel-workpiece contact zone by a power, P, determined as [2]

$$P = \left(\frac{1}{2}\rho R\omega\right) C_s \left(\sum_{k=1}^{n_{cv}} v_{ik}\right)^2, \quad (1)$$

where R is the wheel radius, ρ is the coolant density, and C_s is the coefficient representing the influence of the wheel configuration, defined as

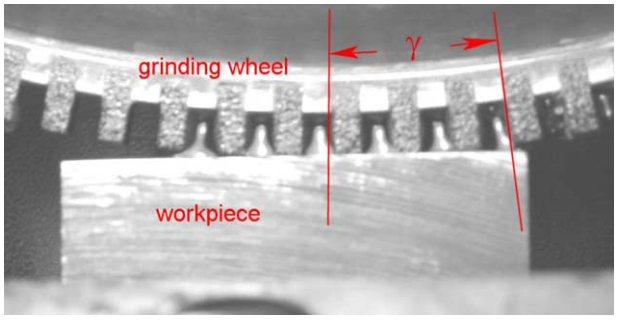

Fig. 1. Penetration of coolant into a grinding zone.

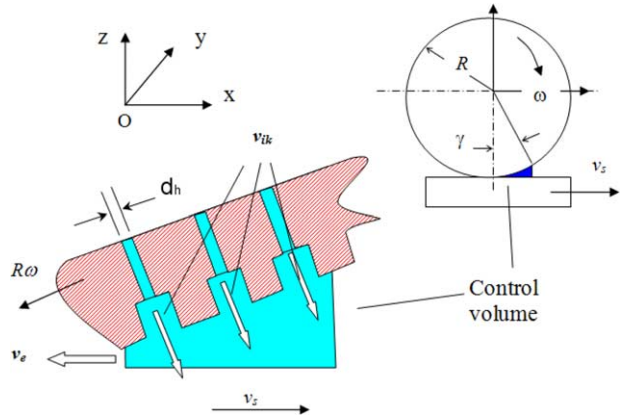

Fig. 2. Analytical control volume.

$$C_s = \frac{1}{b}\left(\frac{\pi d_h^2}{4}\right)^2\left(\frac{2R}{h}-1\right), \tag{2}$$

where b is the wheel width, d_h is the perforated hole diameter, h is the equivalent thickness of a coolant layer in the wheel-workpiece contact zone [2], and n_{cv} is the number of the coolant jets within the control volume, defined as

$$n_{cv} = \frac{N\gamma}{2\pi}, \tag{3}$$

in which N is the total number of the segments fitted in a wheel and γ is the control volume angle, a function of the viscosity, μ, and surface tension, σ, i.e.

$$\gamma = \gamma(\mu, \sigma). \tag{4}$$

In Eq. (1), v_{ik} is the velocity of a coolant jet, which, according to the continuity law, can be expressed in term of the individual flow rate of coolant through a hole, Q_{ik}, as

$$v_{ik} = \frac{4Q_{ik}}{\pi d_h^2}. \tag{5}$$

On the other hand, v_{ik} can be written as, following the energy equation,

$$v_{ik} = v_2 = \left[v_1^2 + 2\Delta_z\left(g + \frac{f_c}{\rho}\right) + \frac{\Delta p}{\rho}\right]^{1/2} \tag{6}$$

where v_1 is the initial velocity at plane 1, $\Delta z = z_1 - z_2$ is the perforated hole length, $\Delta p = p_1 - p_2$ is the pressure drop through a hole (Fig. 3) and $f_c = \rho R\omega^2$ is the centrifugal force acting on a unit coolant volume.

It should be mentioned that to reduce the excessive number of cutting edges and their undesirable friction with the workpiece [2], the segmented wheel is often designed to posses more than one coolant jet within the control volume, i.e. $n_{cv} > 1$, as shown in Fig. 1. However, due to the wheel rotation, the distributions of coolant flow rates, Q_{ik}, and hence the coolant jet velocity v_{ik} over the entire control volume are not uniform, as shown in Fig. 4.

Hence, to obtain a quantitative prediction, the pumping power P should be expressed as

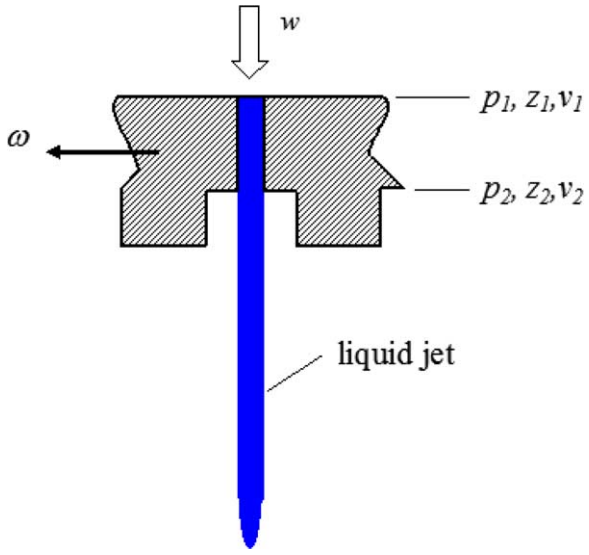

Fig. 3. Flow of a coolant jet.

$$P = P(\rho, \mu, \sigma, R, N, d_h, b, h, \Delta z, \gamma, \omega, \Delta p, v_{ik}) \tag{7}$$

Since the influence of f_c in Eq. (6) has been implicitly taken into account by the combination of ρ, R and ω, the effect of pressure drop Δp can be considered at the static condition where $\omega = 0$. In the case with a coolant chamber as shown in Fig. 5, the equations of Bernoulli and continuity can be applied to planes 1 and 2, to determine the mean static pressure drop, $\Delta\bar{p}_o$, through the perforated holes, which results in [4]

$$\Delta\bar{p}_o = \frac{Q^2\rho}{2}\left(\frac{A_1^2 - A_2^2}{A_1^2 A_2^2}\right) = C_f\left(\frac{Q^2\rho}{2}\right) \tag{8}$$

where Q is the total coolant flow rate supplied to the system and $C_f = (A_1^2 - A_2^2)/A_1^2A_2^2$ is a coefficient representing the influence of the chamber design on $\Delta\bar{p}_o$, in which A_1 and A_2 are the inner cross-sectional area of the fluid chamber and the total cross-sectional area of the perforated holes within the chamber, respectively. If the number of the perforated holes within the chamber is n_{ch} and the internal width of the chamber is b_{ch}, A_1 and A_2 can be derived as

$$A_1 = 2\pi R\frac{n_{ch}}{N}b_{ch}, \tag{9}$$

and

$$A_2 = n_{ch}\frac{\pi d_h^2}{4} \tag{10}$$

Eqs. (8)–(10) can also be applied to the case when coolant is introduced to the wheel by the free-flow method (Fig. 3b). In this case,

$$(n_{ch})_{\text{free-flow}} = N \tag{11}$$

and

$$b_r = b_{ch} \tag{12}$$

where b_r is the width of the inner wheel rim.

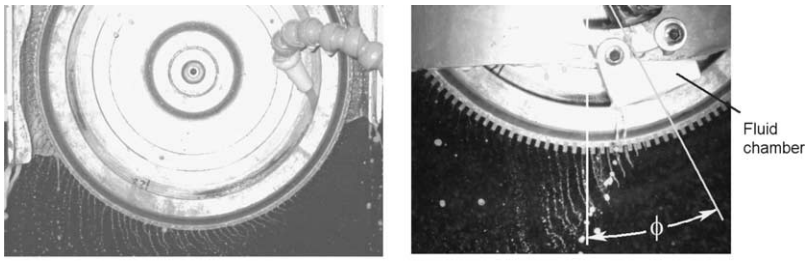

Fig. 4. Coolant flow profiles: (a) free-flow method, and (b) forced flow method.

With the above analytical relationships of the variables in mind, we can simplify Eq. (7) to

$$P = P(\rho, \mu, \sigma, C_f, R, b, h, \omega, Q) \tag{13}$$

Then the Buckingham Π theorem [17,18] allows the relationship to be expressed as

$$f(\pi_1, \pi_2, \pi_3, \pi_4, \pi_5, \pi_6, \pi_7) = 0 \tag{14}$$

where

$\pi_1 = \frac{P}{\rho R^5 \omega^3} = P^*$, is the power number representing the pumping power achieved;
$\pi_2 = \frac{\rho R^2 \omega}{\mu} = \mathrm{Re}$, is the Reynolds number representing the effect of viscosity;
$\pi_3 = \frac{\rho R^3 \omega^2}{\sigma} = \mathrm{We}$, is the Weber number representing the effect of surface tension;
$\pi_4 = C_f R^4$, standing for the influence of method of introducing coolant into the segmented wheel system;
$\pi_5 = \frac{Q}{R^3 \omega} = Q^*$, representing the effect of coolant flow rate supplied to the system;
$\pi_6 = \frac{b}{R}$, representing the effect of wheel width; and
$\pi_7 = \frac{h}{R}$, representing the combination effect of the wheel specification and the grinding depth of cut.

For a given segmented wheel system, π_4, π_6 and π_7 can be reconciled, i.e.

$$\pi_{4,6,7} = \pi_4 \pi_6 \pi_7 = C_f b h R^2 = C_{fw}^* \tag{15}$$

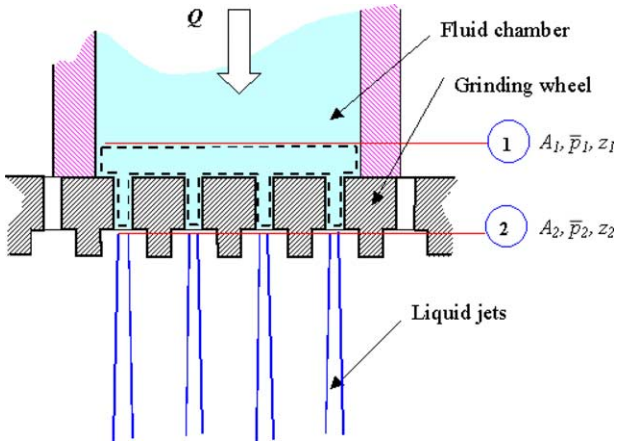

Fig. 5. Schematic of the coolant flow through the holes.

which can be considered as a geometrical influence number to represent the combination effects of π_4, π_6 and π_7 of the system.

Hence, Eq. (14) can be rewritten as

$$P^* = f_1(\mathrm{Re}, \mathrm{We}, C_{fw}^*, Q^*) \tag{16}$$

The power law of dimensional analysis [19] is used to express Eq. (16) in a form,

$$P^* = C_p X_p \tag{17}$$

where C_p is a correlation coefficient, and

$$X_p = \mathrm{Re}^m We^n (C_{fw}^*)^q (Q^*)^r. \tag{18}$$

2.2. Experimental verification

The component of $\left(\sum_{k=1}^{n_{cv}} v_{ik}\right)$ in Eq. (1) can be experimentally determined using the method described in the Appendix at the end of the paper. These values are used to compute the magnitudes of dependent parameter P^* in Eq. (17), which, together with the parameters in Eq. (18), gives the result shown in Fig. 6. Within the range of Re and We covering many practical grinding operations with water-based coolants[1]

$$7.3 \times 10^5 \le \mathrm{Re} \le 4.6 \times 10^6$$

and

$$7.1 \times 10^4 \le \mathrm{We} \le 2.2 \times 10^6, \tag{19}$$

the relation below is obtained using the method of multi-variable regression,

$$P^* = 47.8 \mathrm{Re}^{-0.17} \mathrm{We}^{-0.42} (C_{fw}^*)^{0.25} (Q^*)^{1.02} \tag{20}$$

Eq. (20) is capable for predicting the power number P^*. Since wheel speed ω is included in the dimensionless parameters P^*, Re, We and Q^*, when Eqs. (17) and (18) are rearranged with ω as an explicit variable, a term of $\omega^{0.97}$ will

[1] The maximum and minimum values of Re and We in this range are associated with the grinding conditions below: (a) Wheel speed varies from 6.0 to 28.0 m/s which is 85% of the safety limit using a conventional wheel with high strength CBN vitrified bonded [20]; and (b) The concentration of the water-based coolant (Noritake SA-02) varies from 1:60 to 1:85, whose viscous properties are shown in Table 1.

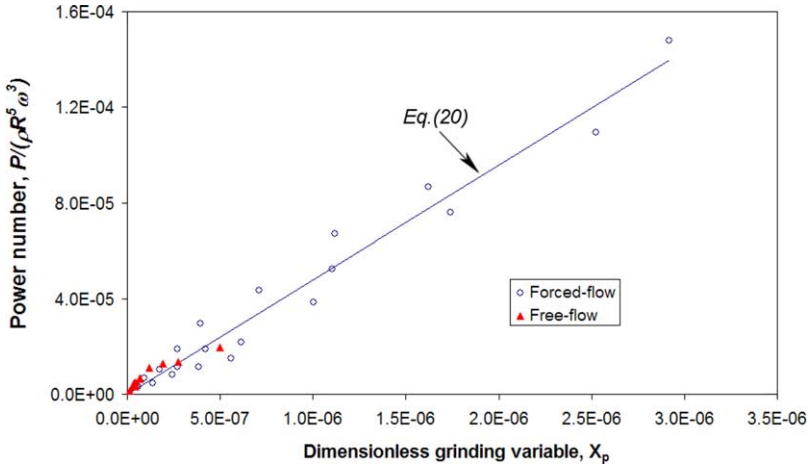

Fig. 6. Pumping power correlation.

appear in the right hand side of Eq. (7). This means that a high wheel speed enhances the pumping power, which is in agreement with the conclusion in Part 1 of this series study [2]. Eq. (20) also shows, by referring to Eqs. (17) and (18), that pumping power is a strong function of the total coolant flow rate ($r=1.02$) and its effectiveness depends very much on the coolant chamber characteristic ($q=0.25$). With a given grinding condition, a higher pumping power can be obtained when coolant is pressurised (un-filled dots in Fig. 6).

3. Practical implications

3.1. Environmental consideration

In the analysis of the mist flow rate generated by a segmented wheel [4], the authors have proposed a formula to predict the mist flow rate ratio Q_m^*, i.e.

$$Q_m^* = \frac{Q_m}{Q} = C_m X_m \tag{21}$$

where

$$C_m = 45.2 \times 10^{-3}$$

and

$$X_m = \mathrm{Re}^{0.06}\mathrm{We}^{0.18}\left(\frac{C_f Q^2}{2\omega^2 R^2}\right)^{0.08}(\cos\phi)^{2.26}$$

in which Q_m is the mist flow rate and ϕ is the angular position of the chamber (Fig. 4b).

The plot of Eq. (21) is illustrated in Fig. 7. In comparison with Eq. (20), it is found that an increase of the coolant viscosity and surface tension, which reduces Reynolds and Weber numbers, will improve coolant penetration and reduce mist. However, the viscous properties depend on the chemical additives in coolant whose use should be minimised in practice to reduce the cost of waste disposal [21,22]. Unfortunately, it can be seen that an adjustment of grinding variables to improve coolant penetration based on Eq. (20) (e.g. increasing ω and Q) will lead to a high mist formation rate according to Eq. (21). Hence, to determine a set of optimal grinding parameters and coolant selection, $(\rho, \mu,\sigma,\omega,Q)_{op}$ that satisfies both the desired mist flow rate and pumping power, Eqs. (21) and (22) must be solved simultaneously, i.e.

$$(\rho,\mu,\sigma,\omega,Q)_{op} = (\rho,\mu,\sigma,\omega,Q)_p \cap (\rho,\mu,\sigma,\omega,Q)_m \tag{22}$$

where $(\rho,\mu,\sigma,\omega,Q)_p$ is the solution of Eq. (20) aiming at the highest pumping power and $(\rho,\mu,\sigma,\omega,Q)_m$ is that of Eq. (21) aiming at the lowest mist flow rate.

To determine the solution of Eq. (22), the constraints must be set based on a given grinding case, which is specified by the limitation of the coolant supply, safety limit of wheel speed, and the limited rate of mist. This will be demonstrated in the example below.

3.2. Example

The grinding conditions are listed in Table 1. With a given grinding wheel system and coolant type, the wheel

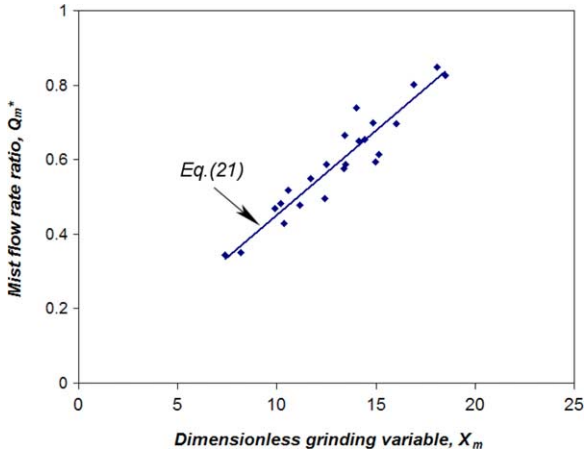

Fig. 7. Mist flow rate correlation.

Table 1
Experimental parameters

Grinding machine	Minini Junior 90 CNC-M286
Grinding wheel	Designation: B100P120V Radius, $R=150$ mm, 144 segments Perforated hole diameter, $d_h=2$ mm Hole length, $(z_1-z_2)=5$ mm Allowable wheel speed = 28.1 m/s
Fluid chamber	Cross sectional area, $A_1=88.3$ mm^2 Number of perforated holes within the fluid chamber, $n=4$
Grinding parameters	- Specific grinding energy: $u_g=57.5$ J/m^3 [28] - Table speed: 5 mm/s - Depths of cut: 25 μm
Coolant	Noritake SA-02 Coolant density: $\rho=980$ kg/m^3 Density of chemical additive, $\rho_a=975$ kg/m^3 Concentration: 1:60 ($\mu=12.1\times10^{-4}$ Ns/m^2, $\sigma=73.1\times10^{-3}$ N/m) 1:85 ($\mu=8.9\times10^{-4}$ Ns/m^2, $\sigma=73.1\times10^{-3}$ N/m)

speed (ω) and coolant supply flow rate (Q) are the two parameters to be determined for the optimisation. Eq. (22) therefore becomes

$$(\omega, Q)_{op} = (\omega, Q)_p \cap (\omega, Q)_m \tag{23}$$

The grinding constraints are:

$$P \geq P_{min}, \tag{24}$$

$$Q_m \leq Q_{m,max}, \tag{25}$$

and

$$\omega \leq \omega_{max} \tag{26}$$

where P_{min} is the minimum pumping power required for a satisfactory grinding without thermal damage, $Q_{m,max}$ is the maximum mist flow rate allowed by an environmental legislation and ω_{max} is the safety limit of rotational wheel speed.

The minimum pumping power required for grinding of 1045 steel at depth of cut = 25 μm has been given in Part 1 of this study [2], i.e. $P_{min}=1.25$ W.

On the other hand, according to the National Occupational Health and Safety Commission (NOHSC) [23], the contamination of inspirable particles in the atmospheric air must not exceed an occupational exposure standard, OES = 5 mg/m^3.

Based on this, the maximum allowable mist flow rate can be found to be $Q_{m,max}=3.1\times10^{-5}$ m^3/s, using the methods given by Refs. [6,23,24]. In the calculation, it was assumed that the ventilation rate of the grinding room was 0.047 m^3/s, which is similar to that of an ordinary kitchen [25], the reference period of mist sampling was 8 h, and the volume of the grinding room was 500 m^3.

With the P_{min} and $Q_{m,max}$ ready above, it is now possible to determine $(\omega, Q)_{op}$ in Eq. (23). By substituting the value of P_{min} into Eq. (20), a minimum coolant flow rate, Q_{min}, can be determined. At the same time, the maximum coolant flow rate Q_{max} controlled by Eq. (21), can also be determined by substituting the value of $Q_{m,max}$. The optimised flow rate must be within the range

$$Q_{max} \geq Q \geq Q_{min}, \tag{27}$$

to ensure a sufficient coolant quantity for the satisfactory grinding and a mist flow rate below the limit. The calculation procedure is shown Fig. 8.

Some numerical results are listed in Table 2. It appears that when a wheel speed is below 1200 rpm, $Q_{max} < Q_{min}$.

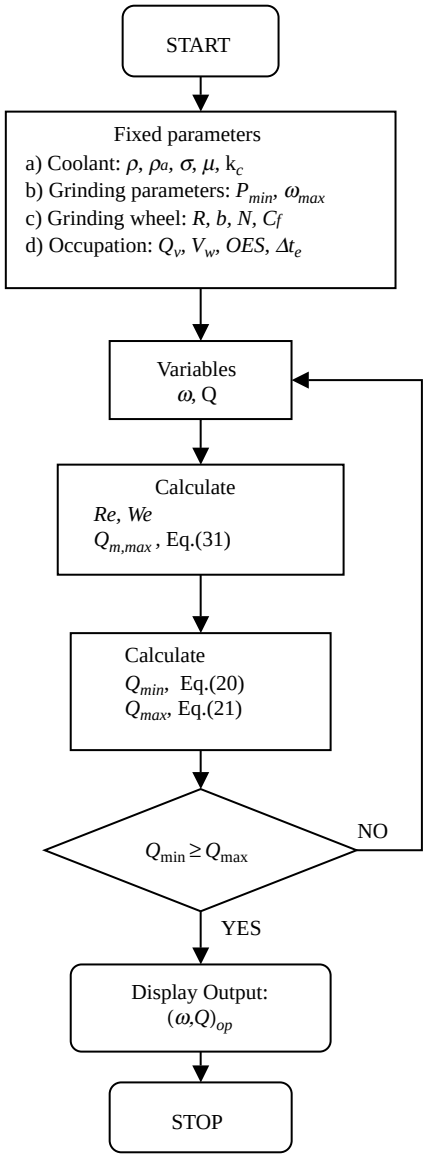

Fig. 8. Optimisation process.

Table 2
Optimisation results

ω (rpm)	Re ($\times 10^6$)	We ($\times 10^5$)	Q_{min} (L/min)	Q_{max} (L/min)
700	1.3	2.4	5.4	3.5
1000	1.9	5.0	3.8	3.2
1200	2.3	7.1	3.2	3.1
1450	2.8	10.4	2.7	3.0
1785	3.4	15.8	2.2	2.8

This is not reasonable and indicates that in this case, a higher ventilation rate must be provided to remove the harmful mist more quickly. The optimal condition $(\omega, Q)_{op}$ is found to be $\omega = 1785$ rpm at which $Q_{max} = 2.8$ L/min being slightly higher than $Q_{min} = 2.2$ L/min, indicating that the operation consumes less coolant.

The above optimisation process can be also applied to different selections of coolant types with Re and We numbers in the valid range.

3.3. Conclusions

A parametric model has been developed to predict the power of coolant penetration into the grinding zone with the application of a segmented wheel. Experimental data were found to be in reasonable agreement with the prediction.

By coupling with the mist formation analysis, the developed model offers a control guideline for the optimal use of grinding coolants in achieving a balanced consideration of process productivity and environmental consciousness.

Acknowledgements

This work was supported by the Australia Research Council (ARC). The authors appreciate very much Mr. Y. L. Pai and Mr. J. Huang at Kinik Grinding Wheel Corp. for making the wheel segments.

Appendix

Determination of v_{ik}

According to the Weber theory [6,8] for the instability of Newtonian jets, when a liquid jet subjected to the forces of surface tension and inertia,

$$\frac{l}{d_1} = \ln\left(\frac{d_1}{2\delta}\right) \mathrm{We}_l^{0.5}(1 + 3\mathrm{Oh}) \tag{A1}$$

where δ is the amplitude of disturbance; l and d_l are the break-up length and diameter of a liquid jet, respectively (Figs. 4a and b) which can be determined using the method of high speed strobe photography [4]; We and Oh is the Weber and Ohnesorge number, respectively, defined as

$$\mathrm{We}_l = \frac{\rho d_l v_{ik}^2}{\sigma} \tag{A2}$$

$$Oh = \frac{\mu}{(\rho\sigma d_l)^{0.5}} \tag{A3}$$

The parameter $\ln(d_l/2\delta)$ depends on the nature of the jet, i.e. laminar or turbulent, which is determined by the following conditions [26]:

$\mathrm{Re}_l < \mathrm{Re}_c$: laminar flow
$\mathrm{Re}_l > \mathrm{Re}_c$: turbulent flow

where

$$\mathrm{Re}_l = \frac{\rho v_{ik} d_l}{\mu} \tag{A4}$$

and Re_c is the critical Reynolds number, defined as

$$\mathrm{Re}_c = 1.2 \times 10^4 \left(\frac{1}{d_l}\right)^{-0.3}. \tag{A5}$$

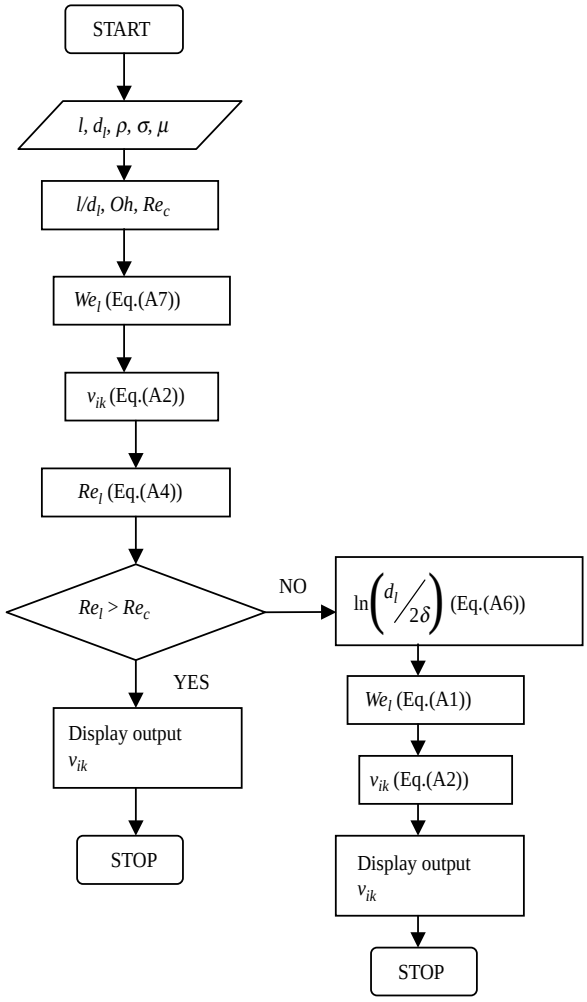

Fig. A1. Steps for determining of v_l.

For a laminar flow, according to Grant et al. [27]:

$$\ln\left(\frac{d_l}{2\delta}\right) = 7.68 - 2.66\mathrm{Oh}, \tag{A6}$$

but for a turbulent flow, Eq. (A1) becomes [27]

$$\frac{l}{d_l} = 8.51\mathrm{We}_l^{0.32} \tag{A7}$$

Now, v_{ik} can be determined following the steps shown in Fig. A1.

References

[1] A.S. Lavine, A simple model for convective heat transfer during the grinding process, Journal of Engineering for Industry 110 (1988) 1–6.

[2] T. Nguyen, L.C. Zhang, The coolant penetration in grinding with segmented wheels—part 1: Mechanism and comparison with conventional wheels, International Journal of Machine Tools and Manufacture 45 (12–13) (2005) 1412–1420.

[3] L.C. Zhang, T. Nguyen, B. Oliver, A grinding wheel assembly and a method of grinding, Patent Application no. 20044901614, Australia.

[4] T. Nguyen, L.C. Zhang, Modelling of the mist formation in a segmented grinding wheel system, International Journal of Machine Tools and Manufacture 45 (1) (2005) 21–28.

[5] L. Preziosi, D. Joseph, The run-off condition for coating and rimming flows, Journal of Fluid Mechanics 187 (1988) 99–133.

[6] L. Bayvel, Z. Orzechowski, Liquid Atomization, Combustion—An International Series, Taylor and Francis, London, 1993.

[7] A.H. Lefebvre, Atomization and Spray Combustion—An International series, Hemisphere Pub. Corp., New York, 1989.

[8] M.J. McCarthy, Molloy, Review of stability of liquid jets and the influence of nozzle design, The Chemical Engineering Journal 7 (1) (1974) 1–20.

[9] I.A. Greaves, Respiratory health of automobile workers exposed to metal working fluid aerosols: respiratory symptoms, American Journal of Industrial Medicine 32 (5) (1997) 450–459.

[10] N.A. Fleck, K.L. Johnson, M. Mear, C. Zhang, Cold rolling of thin foil, Journal of Engineering Manufacture, IMechE B206 (1992) 119–131.

[11] L.C. Zhang, On the mechanism of cold rolling thin foil, International Journal of Machine Tools and Manufacture 35 (1995) 363–372.

[12] L.C. Zhang, T. Suto, H. Noguchi, T. Waida, Applied mechanics in grinding, Part III: a new formula for contact length prediction and a comparison of available models, International Journal of Machine Tools and Manufacture 33 (4) (1993) 587–597.

[13] L.C. Zhang, T. Suto, H. Noguchi, T. Waida, An overview of applied mechanics in grinding, Manufacturing Review 5 (4) (1992) 261–273.

[14] L.C. Zhang, T. Suto, H. Noguchi, T. Waida, Applied mechanics in grinding, Part II: modelling of elastic modulus of wheels and interface forces, International Journal of Machine Tools and Manufacture 33 (1993) 245–255.

[15] J. Sun, L.C. Zhang, Y.-W. Mai, S. Payor, M. Hogg, Material removal in the optical polishing of hydrophilic polymer, Journal of Materials Processing Technology 103 (2000) 230–236.

[16] T.X. Yu., L.C. Zhang, Plastic Bending: Theory and Applications, World Scientific, Singapore, 1996.

[17] P. Gerhart, R. Gross, J. Hochstein, Fundamentals of Fluid Mechanics, Second ed., Addison-Wesley Publishing Company, Reading, MA, USA, 1992.

[18] R.H. Sabersky, A.J. Acosta, E.H. Hauptmann, Fluid Flow: A First Course in Fluid Mechanics, Third ed., Macmillan Publishing Company, New York, 1971.

[19] S. Matsumoto, Y. Takashima, Atomization characteristics of power law fluids by rotating disks, in: The 1st International Conference on Liquid Atomization and Spray Systems (ICLAS'78), Tokyo, Japan, 1978.

[20] Handbook on grinding, Norton Abrasives, Pty.htd, Australia 1992.

[21] M.C. Shaw, Principles of Abrasive Processing, Oxford University Press, Oxford, 1996.

[22] S. Malkin, Grinding Technology—Theory and Applications of Machining with Abrasives, Ellis Horwood Ltd, Chichester, 1989.

[23] National Occupational Health and Safety Commission, Documentation of the Exposure Standards. NOHSC:3008(1995), Government Publishing Service, Canberra, 1995.

[24] Y. Yue, J.W. Sutherland, W.W. Olson. Cutting fluid mist formation in machining via atomization mechanisms, in: Proceedings of the 1996 ASME International Mechanical Engineering Congress and Exposition, ASME, NY, USA, Atlanta, GA, USA, 1996.

[25] The American Society of Heating, Refrigeration and Air-Conditioning Engineering (ASHRAE). Standard 62-1999, "Ventilation for Acceptable Indoor Air Quality".

[26] E. van de Sande, J.M. Smith, Jet breakup and air entrainment by low velocity turbulent jets, Chemical Engineering Science 31 (3) (1976) 219–224.

[27] R.P. Grant, S. Middleman, Newtonian jet stability, Journal for the American Institute of Chemical Engineers (A.I.Ch.E) 12 (4) (1966) 669–678.

[28] L.C. Zhang, T. Suto, H. Noguchi, T. Waida, A study of creep-feed grinding of metallic and ceramic materials, Journal of Materials Processing Technology 48 (1–4) (1995) 267–274.